American Mineralogist, Volume 75, pages 150–162, 1990

Structural variation associated with compositional variation and order-disorder behavior in anorthite-rich feldspars

R. J. Angel
Department of Geological Sciences, University College London, Gower Street, London, WC1E 6BT, England, and Department of Crystallography, Birkbeck College, Malet Street, London, WC1E 7HX, England

M. A. Carpenter
Department of Earth Sciences, University of Cambridge, Downing Street, Cambridge, CB2 3EQ, England

L. W. Finger
Geophysical Laboratory, Carnegie Institution of Washington, 2801 Upton Street, N.W., Washington D.C. 20008, U.S.A.

Abstract

Full structure refinements, based upon single-crystal X-ray diffraction data, have been completed upon a suite of natural and heat-treated anorthite-rich feldspars with compositions between $An_{68}Ab_{32}$ and An_{100}. The complete set of twenty refinements provides an internally consistent database for the detailed characterization of the structural variations arising from changes in composition and cation order. Some of the structural effects reported in the literature are shown to be dependent upon the model chosen to represent the anorthite structure.

Multiple regression analysis has been used to demonstrate how observed tetrahedral T-O bond lengths reflect not only (Al,Si) occupancies, but are perturbed by M-O bonding, T-O-T bond angles, and a linkage factor dependent upon neighboring tetrahedral sites. When the influence of these external factors is removed, the sizes of the tetrahedra, as measured by the mean bond lengths ⟨T-O⟩, exhibit significantly different trends from those associated with uncorrected raw ⟨T-O⟩ bond lengths; previous interpretations of the structures of $I\bar{1}$ feldspars in terms of "anorthite-like" and "albite-like" portions of structure are shown to be simplifications.

Differences in mean bond lengths between tetrahedra are used to define a thermodynamic order parameter, Q_{OD}, for the $C\bar{1}$–$I\bar{1}$ transition. This order parameter can be put on an absolute scale by use of data from end-member albites and anorthites and is used to characterize the states of order of all of the samples studied. Refined thermal parameters of both the large cation sites and those atoms forming the tetrahedral framework result in probability ellipsoids that are oriented in the same way as those obtained from average structure determinations of $P\bar{1}$ structures, even at compositions for which the c and d reflections characteristic of $P\bar{1}$ symmetry are either very diffuse or absent. Whether this implies that all $I\bar{1}$ structures have local $P\bar{1}$ symmetry and a space average is observed by X-ray diffraction, or whether the more albite-rich crystals are displaying large-amplitude vibrational modes that parallel the displacements associated with a $I\bar{1}$–$P\bar{1}$ transition (a time average), cannot be determined by X-ray diffraction experiments.

Introduction

Plagioclase feldspars are among the most abundant minerals within the Earth's crust and are involved in many important igneous and metamorphic reactions. Their undoubted potential for geothermometry and geobarometry has not yet been fully realized, however, because of the remarkably diverse and complex subsolidus behaviour that they exhibit. In particular, natural crystals can develop five distinct diffraction symmetries arising from four commensurate phases and two incommensurate phases, each of which can display a variable degree of (Al,Si) order. Recent developments in the application of Landau theory (e.g., Salje, 1985, 1987; Salje et al., 1985; Redfern and Salje, 1987; Redfern et al., 1988; Carpenter, 1988) have provided a theoretical framework that should allow a proper thermodynamic description of these order-disorder processes to be made. The essential feature of the Landau approach is the use of macroscopic order parameters to characterize the degree of structural change associated with individual phase transitions, and the identification of the manner in which order parameters associated with different phase transitions can interact. In principal, these order parameters may be defined without knowledge of the details of how the structures evolve on an atomic scale. In practice, however, detailed struc-

0003–004X/90/0102–0150$02.00

ture observations can be highly informative as to the mechanisms of the atomic processes involved and may also be essential for placing the macroscopic order parameters on an absolute scale.

Progress in dealing with the thermodynamics of the plagioclase feldspar solid solution is being achieved by first treating each structural phase transition separately. In this context the $C\bar{1}$–$I\bar{1}$ transition, which is due primarily to (Al,Si) ordering, is perhaps the most important as it divides the solid solution into two separate segments over a very wide temperature range (Carpenter and McConnell, 1984). Until now, the order parameters for $I\bar{1}$ crystals have only been determined indirectly through lattice-parameter measurements and calorimetric determinations of the enthalpy changes associated with ordering (Carpenter et al., 1985; Carpenter, 1988). Such measurements provide a relative measure of the order parameter, Q_{OD}, and although ^{29}Si NMR results (Kirkpatrick et al., 1987) place some constraints on its magnitude, only determinations of the structures of feldspars can provide numerical values that are sufficiently accurate for testing the Landau approach. Unfortunately, the uncertainties introduced into the structural data by differences in data collection and refinement procedures in different laboratories are sufficient to confuse the trends in Q_{OD} values that may be derived from published structure refinements. We have therefore undertaken an X-ray diffraction study of a suite of natural anorthite-rich plagioclase feldspars ranging in composition from $An_{100}Ab_0$ to $An_{68}Ab_{32}$. In addition to following structural variations with composition, the effect of temperature has been investigated by refining the structures of some of these crystals after they had been annealed at temperatures between ~1300 °C and ~1535 °C to induce partial (Al,Si) disorder. The resulting database of 20 refined structures presented in this paper provides the high internal precision necessary to determine absolute measures of Q_{OD} and to evaluate variations in the state of order of $I\bar{1}$ feldspars. In subsequent papers, these evaluations of Q_{OD} will be used to analyze the thermodynamics of ordering within the $I\bar{1}$ solid solution.

Experimental details

All of the feldspars used in this study were separated from natural rocks and have been described by Carpenter et al. (1985). Some of the single crystals were taken from the actual powders used by Carpenter et al. (Val Pasmeda, Monte Somma, Monte Somma/1, 115082a/1, 87975a, 87975a/1, 21704a, 21704a/1, 101377a, 101377a/1, Crystal Bay, Lake Co.). Each of these samples was subjected to heating in air for ~12 h at ~800 °C during the process of purification for the calorimetric measurements. The high-temperature annealing was carried out upon ~0.4 g of powder wrapped in Pt foil sitting in a Pt bucket, and quenching was achieved by manually removing the bucket from the furnace and allowing it to cool in air. Sample 115082a was from the same density separate as the material used for calorimetry, but had not been heated at 800 °C. The remaining crystals (Val Pasmeda/3–/8 and Monte Somma/6–/8) were heat treated specifically for this study at temperatures of 1350–1535 °C, following the same procedure as for the calorimetry samples, except that only a few milligrams of each powder were used. Nominal compositions and annealing conditions are specified in Table 1. It should be noted, however, that each powder showed a small range of composition (see Carpenter et al., 1985). In terms of the simple classification of structural state (Kroll, 1983), most of the natural samples are "low," whereas their heat-treated equivalents are "high" (see Fig. 2 of Carpenter et al., 1985).

Single crystals free of inclusions and obvious twinning were selected from each sample and were mounted in the conventional manner for X-ray diffraction. Prior to data collection, each crystal was checked for diffraction quality and absence of twinning on the basis of ω scans of several diffraction maxima. Several crystals were rejected on this criterion, even though no twinning was detectable optically. It should be noted that even the best crystals from the heat-treated samples exhibited noticeably poorer diffraction quality in terms of peak widths than those of the natural samples, as predicted from Landau theory (Salje and Wruck, 1988).

All of the crystals exhibited sharp reflections of class *a* ($h + k$ even, l even) and class *b* ($h + k$ odd, l odd), which alone are indicative of *I*-lattice symmetry. In addition, the three most anorthite-rich natural samples (Val Pasmeda, Monte Somma, and 115082a) possess the *c* and *d* reflections characteristic of $P\bar{1}$ symmetry. A number of the other samples show diffuse intensities at the positions of *c* reflections in electron-diffraction patterns (Carpenter et al., 1985), but these proved to be too diffuse and weak to be collected by conventional diffractometer techniques. Data collections were carried out with a Rigaku AFC5 diffractometer equipped with a rotating anode X-ray source that provided Mo$K\alpha$ radiation, operated typically at 50 kV and 180 mA. Data were collected in a constant-precision mode with continuous $\omega - 2\theta$ scans and with a scan width determined empirically from observed diffraction profiles from each crystal. Intensities were corrected for Lp effects and absorption (μ_l ranged from 14 to 16 cm^{-1}) and reduced to structure factors with a modified version of the program of Burnham (1966). After data collection, each crystal was transferred to a Picker four-circle diffractometer equipped with a conventional Mo X-ray tube [$\lambda(K\alpha_1) = 0.7093$ Å]. Unit-cell parameters (Table 1) were determined by vector least-squares fit to the positions of between 15 and 20 reflections in the range $35° < 2\theta < 45°$ centered by using the eight-position technique of King and Finger (1979) to eliminate zero and centering errors.

Structure refinements were carried out with the least-squares program RFINE88, a development version of RFINE4 (Finger and Prince, 1975). Each reflection was assigned a weight of $w = [\sigma^{-2}(F_o)]$, where $\sigma(F_o)$ is the error derived from counting statistics, and the function minimized was $\Sigma\, w(|F_o| - |F_c|)^2$. Reflections with $F_o < 3\sigma_F$ were ex-

TABLE 1. Crystal data for anorthites refined in this study (see Carpenter et al., 1985, for further description)

	Val Pasmeda	Monte Somma*	115082a	87975a	21704a	101377a	Crystal Bay
n_{An} (mol% An)	100	98	96	89	86	78	72
a (Å)	8.175(1)	8.1796(5)	8.178(2)	8.178(1)	8.1824(5)	8.174(2)	8.174(4)
b (Å)	12.873(1)	12.8747(8)	12.870(3)	12.869(1)	12.8740(6)	12.866(3)	12.880(6)
c (Å)	14.170(1)	14.172(1)	14.175(3)	14.178(1)	14.192(1)	14.187(3)	14.200(5)
α (°)	93.11(1)	93.134(6)	93.17(2)	93.30(1)	93.335(4)	93.43(2)	93.50(3)
β (°)	115.89(1)	115.885(5)	115.97(1)	116.02(1)	116.057(4)	116.04(1)	116.11(3)
γ (°)	91.28(1)	91.236(5)	91.15(2)	90.97(1)	90.860(4)	90.69(2)	90.55(4)
V (Å^3)	1337.8(2)	1339.0(2)	1337.7(5)	1337.1(1)	1339.4(1)	1337.0(5)	1338.8(9)
Space group	$P\bar{1}$	$P\bar{1}$	$P\bar{1}$	$I\bar{1}$	$I\bar{1}$	$I\bar{1}$	$I\bar{1}$
$P\bar{1}$ refinements							
R	3.4	6.9	6.4				
R_w	2.8	4.7	7.9				
N_{par}	470	470	470				
N_{obs}	3257	4333	4939				
$I\bar{1}$ refinements							
R	4.8	5.4	4.4	5.0	5.1	3.7	6.9
R_w	3.7	3.8	4.0	4.2	3.9	3.0	5.3
G_{fit}	1.3	1.4	1.8	1.4	1.5	1.6	1.3
N_{par}	257	257	257	257	256	256	257
N_{obs}	2716	2611	2975	2480	2688	3008	1951

	Lake Co.	Val Pas-meda/3	Val Pas-meda/6	Val Pas-meda/7	Val Pas-meda/8	Monte Somma/1*	Monte Somma/6
n_{An} (mol% An)	68						
T_{anneal} (°C)	—	1350 ± 5	1533 ± 5	1471 ± 3	1413 ± 4	1306 ± 4	1533 ± 5
Anneal time (d)		21	2.74	7	30.71**	21	2.74
a (Å)	8.173(1)	8.177(1)	8.181(1)	8.182(1)	8.180(1)	8.183(1)	8.185(1)
b (Å)	12.869(1)	12.867(2)	12.864(2)	12.869(1)	12.873(2)	12.874(1)	12.869(1)
c (Å)	14.200(1)	14.170(2)	14.167(2)	14.169(1)	14.167(2)	14.176(1)	14.173(1)
α (°)	93.46(1)	93.19(1)	93.26(1)	93.24(1)	93.21(1)	93.17(1)	93.25(1)
β (°)	116.06(1)	115.83(1)	115.77(1)	115.77(1)	115.79(1)	115.85(1)	115.78(1)
γ (°)	90.54(1)	91.24(1)	91.18(1)	91.21(1)	91.25(1)	91.23(1)	91.15(1)
V (Å^3)	1338.1(1)	1338.1(3)	1338.7(3)	1339.6(2)	1339.3(4)	1340.1(2)	1340.5(2)
Space group	$I\bar{1}$	$I\bar{1}$	$I\bar{1}$	$I\bar{1}$	$I\bar{1}$	$I\bar{1}$	$I\bar{1}$
R	4.8	6.1	6.2	5.1	4.9	4.4	5.3
R_w	3.9	4.7	4.6	4.0	3.8	3.1	3.6
G_{fit}	1.7	1.3	1.4	1.3	1.3	1.5	1.4
N_{par}	257	257	256	256	257	256	256
N_{obs}	2497	2235	2136	2476	2591	2889	2530

	Monte Somma/7	Monte Somma/8	115082a/1	87975a/1	21704a/1	101377a/1
T_{anneal} (°C)	1471 ± 3	1413 ± 4	1306 ± 4	1300 ± 10		
Anneal time (d)	7	30.71**	21	21	—†	—†
a (Å)	8.186(1)	8.174(4)	8.176(2)	8.175(2)	8.1808(4)	8.174(2)
b (Å)	12.870(1)	12.860(3)	12.867(3)	12.854(3)	12.8740(7)	12.870(3)
c (Å)	14.175(2)	14.166(4)	14.170(2)	14.163(3)	14.1895(8)	14.184(3)
α (°)	93.26(1)	93.21(2)	93.22(1)	93.32(2)	93.378(5)	93.45(2)
β (°)	115.80(1)	115.80(2)	115.83(1)	115.90(1)	115.926(3)	115.96(1)
γ (°)	91.16(1)	91.17(4)	91.19(2)	90.97(2)	90.837(4)	90.67(2)
V (Å^3)	1340.8(2)	1336.8(8)	1337.9(5)	1335.1(5)	1340.3(1)	1337.9(5)
Space group	$I\bar{1}$	$I\bar{1}$	$I\bar{1}$	$I\bar{1}$	$I\bar{1}$	$I\bar{1}$
R	5.7	5.4	4.9	5.8	5.3	4.8
R_w	4.3	4.2	3.4	4.3	4.2	3.3
G_{fit}	1.4	1.3	1.4	1.3	1.6	1.6
N_{par}	256	256	256	257	256	256
N_{obs}	2441	2457	2574	2223	2435	2245

Note: Nominal composition = n_{An}. Numbers in parentheses are the estimated standard deviations (1σ) in the last decimal place given. This convention applies to all subsequent tables.

* Two typographical errors are present in Carpenter et al. (1985): In Table 3 (lattice parameters) the labels Monte Somma and Monte Somma/2 should be exchanged, and in Table 4 the annealing temperature of Monte Somma/1 should be 1306 °C rather than 1360 °C as given.

** Includes a brief spell at room temperature after ~10 d, due to furnace failure.

† Samples annealed at 1366 ± 8 °C for 23 d, followed by 21 d at 1306 ± 4 °C.

cluded from the refinements. Complex atomic scattering factors for neutral atoms were taken from the *International Tables for X-ray Crystallography* (1974). Extinction effects were corrected with the Becker and Coppens (1974) formalism (isotropic Lorentzian type I distribution); when g refined to less than its esd, its value was fixed at zero. The details of the structure models that were refined are described and discussed in detail in the following sections. Final agreement indices from all of the refinements are reported in Table 1, atomic coordinates and temperature factors in Table 2, bond lengths in Tables 3 and 4, and bond angles in Table 5.[1]

Results

Extensive reviews of the structures of plagioclase feldspars can be found in Ribbe (1983) and Smith and Brown (1988). It is useful to recall that the site nomenclature of Megaw (1956) (here modified in the manner of Prewitt et al., 1976, for ease of typesetting) was devised to indicate which sets of sites become symmetrically equivalent in higher-symmetry feldspar structures. For example, those sites whose labels differ by the symbol "i" in the $P\bar{1}$ structure become equivalent under $I\bar{1}$ symmetry, whereas those whose labels differ by "z" become equivalent on further increase of symmetry to $C\bar{1}$ (with the c axis $\approx$ 7 Å).

The purpose of this study was to provide a structural database for the examination of the cation ordering–cation disordering behavior of feldspars with $I\bar{1}$ symmetry. However, anorthite-rich feldspars undergo a displacive phase transition at low temperatures and pressures to a structure with $P\bar{1}$ symmetry. In our study, the three most anorthite-rich natural crystals exhibited $P\bar{1}$ diffraction symmetry at room temperature and pressure, and, for reasons that will become apparent, our discussion of the structural variation in the $I\bar{1}$ phase must start with an analysis of the $P\bar{1}$ structures.

$P\bar{1}$ structures

The structure of a $P\bar{1}$ anorthite was first determined by Kempster et al. (1962), who analyzed data collected from a sample from Monte Somma (An_{97}–An_{100}). The features of the structure were subsequently confirmed in an analysis of end-member Val Pasmeda anorthite by Wainwright and Starkey (1971). Other data sets have since been collected on samples of varying compositions with up to 6 mol% albite component (Wenk and Kroll, 1984; Smyth, 1986). Beyond this composition the c and d reflections characteristic of $P\bar{1}$ symmetry become too diffuse to collect reliably by diffractometer methods (Berking, 1976), although attempts have been made to refine $P\bar{1}$ structures to data sets with a and b reflections alone. These will be reviewed in a later section.

The feldspar structure consists of a framework of corner-linked tetrahedra that contain Al and Si atoms. Outside of this framework there are sites for larger alkali and alkaline-earth cations. These extraframework sites are designated "M" sites ("A" sites in some papers), and in end-member anorthite they are exclusively occupied by Ca. The coordination polyhedra of these sites resemble cubes with a corner missing (two in the case of Mooo), and although the large cations are often regarded as residing in a large cavity, the M-O distances are comparable to other, more regular environments, and the cations are quite tightly bound (Megaw et al., 1962). Indeed, the cage of oxygen atoms around each of the M sites is sufficiently collapsed to make the transfer of any M cation to a position $z + \frac{1}{2}$ sterically impossible.

A number of models for the M sites have been used in previous refinements. Kempster et al. (1962), in the original determination of the $P\bar{1}$ structure, chose to model each M site as a single isotropic Ca atom, an approach subsequently used (with anisotropic atoms) both here and by Wainwright and Starkey (1971). Such models result in highly anisotropic thermal ellipsoids for the cations in the Mooo and Mzio cavities; this result has led some workers either to refine these two sites alone as split positions (Smyth, 1986) or to split all four M positions (Wenk and Kroll, 1984). We found that refinements of the Val Pasmeda anorthite that treated the Mooo and Mzio sites as isotropic split atoms converged to slightly better R values than the anisotropic single sites. However, all split-site refinements suffer from such severe correlations between positional parameters, occupancies, and thermal parameters that it is difficult to interpret the results in any reliable way, except to say that all of the various models reflect some smearing-out of the potential well of these sites. This problem is exacerbated in refinements of anorthites with an albite component in solid solution, and by the additional possibility of the presence of M site vacancies (Smyth, 1986). We believe that the resultant correlations between (Ca,Na) occupancy parameters and other structural variables make the direct determination of (Ca,Na) distribution unreliable. Neither do the site sizes provide an unambiguous guide. All three of our refinements show the mean M-O bond length of each site, ⟨M-O⟩, to increase in the order Mooo, Mzoo, Moio, Mzio (Table 4), in common with the results of Wainwright and Starkey (1971), and also with those of Smyth (1986) and Wenk and Kroll (1984) when the split-site ⟨M-O⟩ values are suitably averaged. This might suggest that the larger Na would preferentially occupy Mzio (as Smyth, 1986, suggested), but no significant increase in ⟨Mzio-O⟩ is either observed or expected considering the low Na:Ca ratio. Smyth (1986) also proposed that further cation ordering among the split positions was possible and that, in the absence of extra diffraction maxima, this would reduce the symmetry to $P1$ with the same size cell. Given the pseudosymmetry of the structure, the statistical tests commonly used to detect the presence or absence of a center of symmetry are not valid, and direct refinement

[1] Copies of Tables 2, 3, 4, and 5 may be ordered as Document AM-90-426 from the Business Office, Mineralogical Society of America, 1625 I Street, N.W., Suite 414, Washington, D.C. 20006, U.S.A. Please remit $5.00 in advance for the microfiche.

of a $P1$ structure is somewhat cumbersome. It would perhaps be better to test the suggestion by way of direct probes of the local M-site environment such as Na NMR and to conclude that for current purposes the structures are suitably approximated by centric symmetries.

Before examining the structural trends within the tetrahedral frameworks of the $P\bar{1}$ structures, it is worthwhile considering the uncertainties that arise from interlaboratory comparisons as opposed to the experimental uncertainties present in results from suites of structures refined in an identical manner to data collected on a single diffractometer. Wenk and Kroll (1984) and Smyth (1986) both refined An_{96} anorthites, and the current study duplicates refinements on crystals from the Val Pasmeda (Wainwright and Starkey, 1971; Kalus, 1978) and Monte Somma (Kempster et al., 1962; Czank, 1973) localities. Comparison of the final structures shows that the determinations of individual T-O bond lengths can vary up to 0.02 Å between refinements, which amounts to 3–4 times the combined esd's. Mean values of the four T-O bond lengths in each tetrahedron, ⟨T-O⟩, typically differ by 0.005 Å, with a maximum recorded difference of 0.015 Å. When converted to tetrahedral site occupancies via, for example, the equation of Kroll and Ribbe (1983), this discrepancy corresponds to a difference in the predicted Al-site population of 0.15. These large differences between refinement results can presumably be attributed to different structural models, especially as already discussed for the M sites, different corrections for absorption and extinction, and different experimental techniques of measuring unit-cell parameters.

There are some features of the tetrahedral framework that are common to all of the published refinements. In $P\bar{1}$ anorthites the Al:Si ratio is close to 2:2, which allows, in principle, almost complete ordering of Al and Si. As a first approximation one would therefore expect that there would be two types of tetrahedra, one containing Al, the other Si, and that within these two groups there should be very little variation in size as measured by ⟨T-O⟩. In addition, since diffusion rates at temperatures below the $I\bar{1}$–$P\bar{1}$ transition (~240 °C for An_{100} and decreasing with increasing albite content) are extremely slow, redistribution of Al and Si under $P\bar{1}$ symmetry is extremely unlikely. Pairs of tetrahedra within the $P\bar{1}$ structure that would be equivalent in $I\bar{1}$ should therefore have identical occupancies and thus the same ⟨T-O⟩ values. However, differences between these $I\bar{1}$-related pairs are always observed and can be largely attributed to different bonding environments of the oxygen atoms (Megaw et al., 1962; Phillips et al., 1973; Wenk and Kroll, 1984). However, this does not account for all of the variation in either individual T-O bond lengths or the ⟨T-O⟩ values of the Al and Si sites, and two further factors appear to be involved. First, the tetrahedral sites may have slightly mixed (Al,Si) occupancies, and indeed some partial disordering is required by thermodynamics. Second, in the case of oxygen atoms bonded to the more diffuse M sites, the refined position may represent an average of two or more real positions and thus not result in any real T-O bond length at all. This certainly seems to be true for the T1ozi tetrahedron (Smyth, 1986), which is by far the largest site in all published refinements.

Over the small composition range spanned by our three $P\bar{1}$ samples, the effect of bonding environment and other factors may not differ by a large amount between corresponding sites in different crystals. It may therefore be significant to note the following structural trends as a function of increasing albite content. Six of the Al-rich tetrahedra show decreases in ⟨T-O⟩, whereas the T1ozo and T1ozi (Al-rich sites) and all eight of the Si-rich tetrahedra remain the same size. These trends are also reflected in a decrease in the grand mean of the T-O bond lengths of the Al-rich sites, ⟨⟨Al-O⟩⟩, and in the grand mean of all of the sites, ⟨⟨T-O⟩⟩. There are no significant changes in the internal geometry (O-T-O angles) of the various tetrahedra, but there is a perceptible decrease in the difference between T-O-T angles that would be equivalent in $I\bar{1}$, especially those whose difference is largest (Obmo, Obmz, Odmo, Odmz pairs). These three $P\bar{1}$ structures therefore show an approach toward $I\bar{1}$ symmetry with increasing albite content, which is consistent with the decreasing temperature of the $I\bar{1}$ to $P\bar{1}$ transition, and the observed diminution of the intensities of the c and d reflections.

$I\bar{1}$ structure models

Two basic types of $I\bar{1}$ structural model may be refined to the a and b reflections alone. Both types have been used in the literature in refinements of those crystals with albite contents in excess of around 10 mol% that exhibit $I\bar{1}$ diffraction symmetry. Although comparisons have frequently been made between the results from the two types of model, tests have not been performed to determine either how well each reflects the true nature of the structure, or whether the results from the two models are really compatible. We have therefore carried out refinements of both of the structural models to the a and b reflections collected from the 115082a crystal. Comparison of the resulting $I\bar{1}$ structures with the $P\bar{1}$ structure obtained by refinement to all four classes of reflections provides a test of the $I\bar{1}$ models and gives us a basis for an understanding of the structures of those more albite-rich crystals that exhibit $I\bar{1}$ diffraction symmetry.

In the "split-atom" $I\bar{1}$ model, each atom of the $P\bar{1}$ structure is replaced by a half-atom, and these half-atoms are then refined subject to $I\bar{1}$ symmetry. In the present study, large correlations were found to develop between the positional parameters of related half-atoms in the refinement that made it totally unstable. Progress could only be achieved by refining half of the atoms (one of each pair) on alternate cycles. Convergence was still not achieved, with positional parameters oscillating on the last cycles by up to 0.5 esd. The ⟨T-O⟩ values from this refinement are compared in Table 6 with those from the full $P\bar{1}$ refinement to all four classes of reflections. Individual ⟨T-O⟩ values differ by up to 0.019 Å between the

split-atom model and the $P\bar{1}$ structure, but the combined means of each pair of tetrahedra do agree quite well. Errors in individual positional parameters of each half-atom in the split model are therefore being partially compensated by the opposite error in the same parameters of its pair, as would be expected from the patterns of high correlations between parameters within the refinements. The resulting split vectors[2] are consequently larger than those in the $P\bar{1}$ structure, and the split-atom $I\bar{1}$ structure also has extremely distorted tetrahedra. For example, the shortest Si-O bond is 1.545 Å compared to 1.583 Å in the $P\bar{1}$ structure, and corresponding individual T-O bonds in the two refinements differ by up to 0.046 Å. Overall, the split-atom model gives a poor representation of the true structure of a $P\bar{1}$ crystal and makes refinements unreliable and slow through high correlations between parameters. The interpretation of such a model is also complicated by the necessary task of the assignment of the members of atom pairs to one half or the other of the unit cell, which can only be done by analogy with a known $P\bar{1}$ structure.

By contrast, the "single-atom" $I\bar{1}$ model consists of replacing each atom pair of the tetrahedral framework with a single anisotropic atom, and the resultant averaging manifests itself in the form of large "thermal ellipsoids." For those atoms corresponding to pairs in $P\bar{1}$ with large split vectors, the major axis of the thermal ellipsoid is oriented parallel (within a few degrees) to the split vector, and the rms displacement corresponding to this "thermal" ellipsoid reflects its magnitude (Fig. 1; see also Bruno et al., 1976). The magnitudes of the split vectors for the M sites in $P\bar{1}$ anorthites are so great that if refinements are attempted in $I\bar{1}$ without modeling each of them as a pair of partially occupied sites, reasonable convergence cannot be obtained. Examination of the refined positions of these M-site half-atoms in this $I\bar{1}$ model shows that they are within 0.03 Å (i.e., within the combined esd's) of the corresponding positions in $P\bar{1}$, with the exception of the Mzio site, which is shifted by some 0.23 Å.

By its nature as an average structure, the single-atom $I\bar{1}$ model cannot be expected to reproduce the framework geometry of the full $P\bar{1}$ structure. In particular, ⟨T-O⟩ values from this model (Table 6) are generally less than those calculated from the pair of corresponding tetrahedra in $P\bar{1}$. Figure 2 demonstrates that this arises from the nature of the averaging. The differences apparent in Table 6 between various models (see also Bruno et al., 1976) also demonstrate that the evaluation of trends in bond lengths, or any other structural parameters, should only be made between structures refined in the same way. For example, the discontinuity in ⟨⟨T-O⟩⟩ with composition noted by Kroll and Ribbe (1983, their Fig. 1) results from the comparison of data from $P\bar{1}$ and $I\bar{1}$ split-atom models for anorthite-rich crystals with data from single-atom $I\bar{1}$ models for crystals with higher albite contents. This discontinuity is clearly not due to some bonding effect involving Ca as Kroll and Ribbe (1983) have suggested.

In the main part of this study, the results of which are described below, the single-atom $I\bar{1}$ model was preferred over the split-atom model because it results in a structure model with fewer parameters, refinement of which converges rapidly. A further advantage is that no prior assumptions need be made concerning the type of averag-

Table 6. Comparison of T-O bond lengths from different refinement models of 115082a

	$P\bar{1}$ model		$I\bar{1}$ split-atom*		$I\bar{1}$ single-atom
	o	i	o	i	
T1oo-Oa1o	1.631(6)	1.635(6)	1.645	1.636	1.634(3)
-Oboo	1.627(6)	1.612(6)	1.639	1.606	1.616(3)
-Ocoo	1.591(6)	1.584(6)	1.545	1.614	1.587(3)
-Odoo	1.627(6)	1.637(6)	1.661	1.613	1.627(3)
Avg.	1.619	1.617	1.623	1.617	1.616
T1oz-Oa1z	1.770(6)	1.771(6)	1.787	1.752	1.762(3)
-Oboz	1.740(6)	1.758(6)	1.736	1.768	1.744(3)
-Ocoz	1.713(6)	1.713(6)	1.722	1.699	1.711(3)
-Odoz	1.759(6)	1.767(6)	1.742	1.782	1.761(3)
Avg.	1.746	1.752	1.747	1.750	1.745
T1mo-Oa1o	1.778(6)	1.763(6)	1.768	1.768	1.765(3)
-Obmo	1.698(6)	1.740(6)	1.696	1.743	1.708(3)
-Ocmo	1.728(6)	1.762(6)	1.729	1.760	1.744(3)
-Odmo	1.745(6)	1.698(6)	1.798	1.659	1.712(3)
Avg.	1.737	1.741	1.748	1.733	1.732
T1mz-Oa1z	1.645(6)	1.647(6)	1.665	1.653	1.646(3)
-Obmz	1.616(6)	1.592(6)	1.611	1.601	1.600(3)
-Ocmz	1.616(6)	1.622(6)	1.595	1.637	1.619(3)
-Odmz	1.586(6)	1.611(6)	1.624	1.581	1.590(3)
Avg.	1.616	1.618	1.624	1.618	1.614
T2oo-Oa2o	1.756(6)	1.754(6)	1.744	1.769	1.748(3)
-Oboo	1.757(6)	1.741(6)	1.741	1.755	1.747(3)
-Ocmz	1.714(6)	1.754(6)	1.730	1.748	1.734(3)
-Odmz	1.687(6)	1.698(6)	1.694	1.699	1.688(4)
Avg.	1.729	1.737	1.727	1.743	1.729
T2oz-Oa2z	1.643(6)	1.628(6)	1.645	1.643	1.635(3)
-Oboz	1.620(6)	1.633(6)	1.625	1.630	1.624(3)
-Ocmo	1.597(6)	1.627(6)	1.684	1.547	1.613(3)
-Odmo	1.622(6)	1.574(6)	1.606	1.590	1.601(3)
Avg.	1.621	1.616	1.640	1.603	1.618
T2mo-Oa2o	1.630(6)	1.648(6)	1.638	1.633	1.639(3)
-Obmo	1.583(6)	1.617(6)	1.592	1.622	1.603(3)
-Ocoz	1.593(6)	1.607(6)	1.602	1.610	1.604(3)
-Odoz	1.650(6)	1.621(6)	1.629	1.629	1.631(3)
Avg.	1.614	1.623	1.615	1.624	1.619
T2mz-Oa2z	1.744(6)	1.765(6)	1.758	1.752	1.754(3)
-Obmz	1.745(6)	1.700(6)	1.757	1.695	1.725(3)
-Ocoo	1.711(6)	1.733(6)	1.674	1.768	1.721(3)
-Odoo	1.739(6)	1.751(6)	1.756	1.751	1.748(3)
Avg.	1.735	1.737	1.736	1.742	1.737
$\langle Si_{rich}\text{-O}\rangle$		1.618		1.620	1.617
$\langle Al_{rich}\text{-O}\rangle$		1.739		1.741	1.736
⟨T-O⟩		1.679		1.681	1.676

* Estimated standard deviations for T-O bond lengths cannot be evaluated for the $I\bar{1}$ split-atom model because only one half of the atom positions were refined on each cycle.

[2] For each atom in the unit cell of a $P\bar{1}$ feldspar at x, y, z, there is a second atom at approximately $\frac{1}{2} + x, \frac{1}{2} + y, \frac{1}{2} + z$ to which it would be symmetrically equivalent under $I\bar{1}$ symmetry. The deviation of the vector between such a pair of atoms from $\frac{1}{2}, \frac{1}{2}, \frac{1}{2}$ is termed the "split vector" and gives a measure of the deviation of the structure from $I\bar{1}$ symmetry. Analogous split vectors can be defined for atom pairs in $I\bar{1}$ structures to describe the deviation from $C\bar{1}$ symmetry.

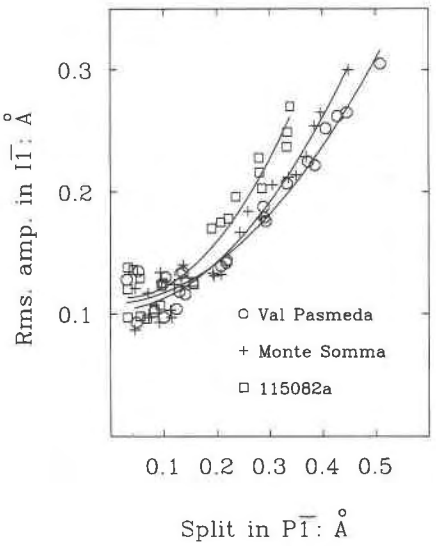

Fig. 1. Comparison of the magnitude of the split vectors (defined in footnote 2) for atom pairs in $P\bar{1}$ refinements with the maximum rms amplitude of the apparent thermal ellipsoid of the corresponding atoms in $I\bar{1}$ refinements. The lines are drawn in to emphasize the general trends in the results.

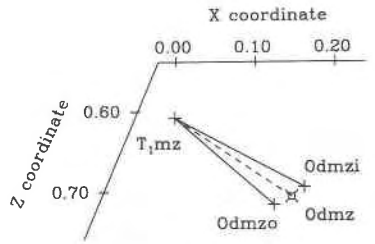

Fig. 2. The relationship between the refined positions and bond lengths of the $P\bar{1}$ and $I\bar{1}$ single-atom models is illustrated by the example of the T1mz-Odmz bond. The crosses on the plan, projected onto (010), indicate the positions of the atoms in the $P\bar{1}$ model (with one set translated by ½, ½, ½). Note that the positions of the two tetrahedral sites are indistinguishable both from one another and from the position given in the $I\bar{1}$ refinement. The Odmz position in the $I\bar{1}$ model lies between the two oxygen positions from the $P\bar{1}$ model; the resulting T-O bond length (dashed line) is clearly shorter than those given by the $P\bar{1}$ model (two solid lines).

ing. Although this averaging is clearly spatial in nature in crystals that exhibit sharp *c* and *d* reflections, it could be either a space or time (i.e., dynamic) average in crystals where these reflections are absent.

$I\bar{1}$ structures

The twenty data sets collected (Table 1) were refined to the single-atom $I\bar{1}$ model described above, including those from the three anorthite-rich crystals that exhibited $P\bar{1}$ diffraction symmetry. Even in the 17 samples that did not display sharp *c* and *d* reflections and that might therefore be assumed to possess true $I\bar{1}$ symmetry, the large cation sites still display a split character and have to be modeled as split sites in order to achieve reasonable convergence of the refinements. The refinement and interpretation of these sites are further complicated by the possibility of (Ca,Na) ordering among them. In this study it was found to be impossible to achieve convergence in refinements of models using separate Na and Ca occupancies. Therefore Ca scattering factors were used throughout for these sites, but with a total population constrained to give a total number of electrons (assuming Ca^{2+} and Na^{+}) appropriate to the composition. These pseudo-Ca occupanices were then refined, and a (Ca,Na) distribution back-calculated by assuming that each pair of sites was fully occupied.

The results are given in the supplement to Table 2. They indicate that, in the relatively well ordered natural samples, the Na content of the Mooo + Moio cavity tends to be greater than that of Mzoo + Mzio. On annealing at elevated temperatures, some redistribution of Na between the two cavities takes place, but whether this is significant given the crudeness of our structural model is difficult to assess. Certainly the distribution of scattering power between the two split sites of each cavity is not deemed to be interpretable especially in view of the high correlations in the refinements between the occupancies, positions, and thermal parameters of the sites. The trends in the average M-O bond lengths are much clearer. As noted by Wenk and Kroll (1984), the ⟨M-O⟩ distances of all four sites decrease with increasing anorthite content, irrespective of the thermal history and state of (Al, Si) order in the sample. Overlain upon this trend is a small increase in ⟨Mooo-O⟩ and ⟨Mzoo-O⟩ after annealing at elevated temperatures (Table 4). The most remarkable feature of the M sites is that the refined positions of all four sites remain almost the same, independent of either composition or thermal history. The split vectors between both "$P\bar{1}$ pairs" (e.g., Mooo and Moio) and "$I\bar{1}$" pairs (e.g., Mooo and Mzoo) therefore remain constant in both magnitude and orientation. The thermal parameters of all four sites (in the form of B_{eq}) do increase significantly with both increasing albite content and after heat treatment (Table 2), and the major axes of the thermal ellipsoids of at least three of the sites (not Mooo) are oriented parallel to the Mooo-Mzoo and Mooo-Moio split vectors. Taken together, these observations suggest that the major minima in the potentials of the M sites, represented by the refined positions, remain the same, but that the potential becomes smeared out with increasing disorder of the tetrahedral framework induced by either thermal treatment or an (Al:Si) ratio that differs from 2:2.

Over the ranges of composition and state of order that we have studied there is very little change, in terms of bond angles, in the overall geometry of the tetrahedral framework. Significant variations are restricted to T-O bond lengths and their means, which are believed to primarily reflect variations in the (Al,Si) occupancies of the various tetrahedra. The grand mean for each structure, ⟨⟨T-O⟩⟩, appears to vary smoothly with composition, but

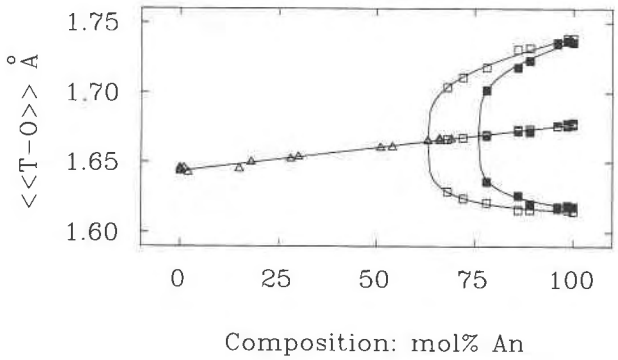

Fig. 3. Grand-mean tetrahedral bond distances, ⟨⟨T-O⟩⟩, in plagioclase feldspars. Squares are data from the 20 $I\bar{1}$ structures refined in this work, and the triangles are values from 19 $C\bar{1}$ structures tabulated by Kroll and Ribbe (1983). The line is that described by Equation 2 in the text. Also shown are ⟨⟨Al-O⟩⟩ and ⟨⟨Si-O⟩⟩ from this work for the natural $I\bar{1}$ crystals (open symbols) and for those annealed at 1300–1370 °C (filled symbols). The trends drawn through these data follow a linear dependence of $(\langle\langle \text{Al-O}\rangle\rangle - \langle\langle \text{Si-O}\rangle\rangle)^4$ on composition.

to be invariant with the state of order (Fig. 3). A linear fit to the 20 data points yields the relation

$$\langle\langle \text{T-O}\rangle\rangle = 0.0357(9)n_{\text{An}} + 1.6419(8). \quad (1)$$

In particular it should be noted that our data do not show the discontinuity around An_{80} reported by Kroll and Ribbe (1983), which arises from differences in the nature of the averaging in various structural models as discussed above. Furthermore, this trend of grand-mean tetrahedral bond lengths in the $I\bar{1}$ structures is continuous with that of the $C\bar{1}$ structures compiled by Kroll and Ribbe (1983). When the 19 $C\bar{1}$ data points (those specimens reported to exhibit a schiller were excluded) are combined with our $I\bar{1}$ data, a linear regression yields

$$\langle\langle \text{T-O}\rangle\rangle = 0.0338(6)n_{\text{An}} + 1.6436(4) \quad (2)$$

with a correlation coefficient, ρ, of 0.997. The most significant deviations from this overall trend occur for one high albite with 7.5 mol% orthoclase component and four end-member low albites. These suggest that at the extreme end of the $C\bar{1}$ solid solution there are some additional factors that perturb the ⟨⟨T-O⟩⟩ values.

In the natural $I\bar{1}$ samples equilibrated at low temperatures, there are two notable trends in the ⟨T-O⟩ of individual tetrahedra over the composition range studied. In the larger Al-rich tetrahedra, all but ⟨T1oz-O⟩ distances decrease continuously with increasing albite content, whereas among the Si-rich tetrahedra the T1oo site exhibits much more expansion than the other three (Fig. 4). The heated samples show a distinctly different pattern; all four Si-rich tetrahedra expand by about the same amount whereas T2oo exhibits significantly less contraction after heating than do the other three Al-rich sites. The T1oz site remains the largest in all of the structures, however. An indication of whether these changes in ⟨T-O⟩ are due to changing occupany alone, or whether they arise as a result of secondary effects such as changes in averaging within the model or other factors, may be obtained by detailed examination of trends in individual T-O bond distances and the factors that contribute to them.

Interpretation of T-O bond lengths

The factors affecting individual T-O bond lengths in aluminosilicates have been well documented. The primary factor is, of course, the (Al,Si) content of the site (e.g., Smith, 1954; Smith and Bailey, 1963). A number of secondary factors have also been shown to be significant:

1. T-O bond lengths are influenced by the (Al,Si) content of the second tetrahedral site to which the oxygen is bonded. Si-O → Si bonds are 0.03 Å longer than Si-O → Al bonds in albites (Phillips and Ribbe, 1973). However, the fact that ⟨⟨T-O⟩⟩ is invariant with Q_{OD} demonstrates that in $I\bar{1}$ feldspars this linkage factor is internally compensated within each individual tetrahedron, as it is in $C\bar{1}$ albites.

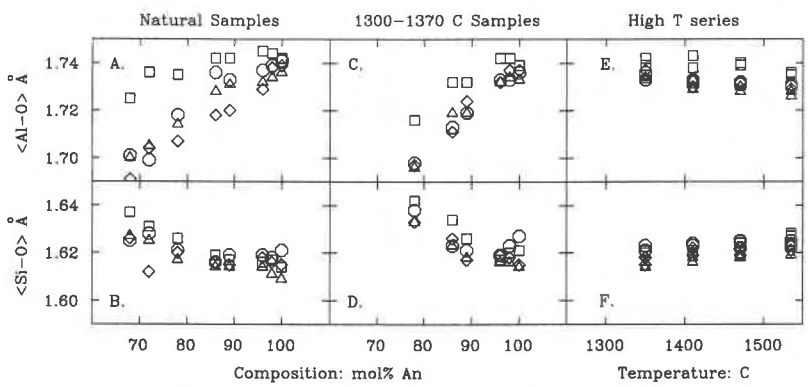

Fig. 4. Variation of mean tetrahedral bond lengths, ⟨T-O⟩, with composition and heat treatment. (**A**, **B**) Trends in natural samples. (**C**, **D**) Trends in samples heat treated at 1300–1370 °C. (**E**, **F**) Variation of ⟨T-O⟩ with annealing temperature for Val Pasmeda and Monte Somma samples. Symbols distinguish the different T sites as follows: □ T1o, △ T1m, ◇ T2o, ○ T2m.

TABLE 7. Regression-analysis results

Term	Coefficient	|T|
$\Sigma - \langle\Sigma\rangle$	0.0952(34)	28.4
$Z[\Sigma - \langle\Sigma\rangle]$	0.0168(47)	3.6
sec(T-O-T) − ⟨sec(T-O-T)⟩	−0.0203(24)	8.6
Z[sec(T-O-T) − ⟨sec(T-O-T)⟩]	−0.0174(34)	5.1
$\langle T_j\text{-O}\rangle - \langle\langle T_j\text{-O}\rangle\rangle$	−0.2199(604)	3.6

Note: Σ is the bond-strength sum from the M cation sites to the oxygen atom calculated in the manner of Wenk and Kroll (1984) and weighted by the (Na,Ca) occupancies given in the supplement to Table 2. $\langle\Sigma\rangle$ is the mean of the four values of Σ over a TO_4 tetrahedron.

Z is a dummy variable, value zero for Si-rich tetrahedra, unity for Al-rich tetrahedra. Thus, for example, the coefficient of $\Sigma - \langle\Sigma\rangle$ is 0.0952 for Si-O bonds and 0.0952 + 0.0168 = 0.1120 for Al-O bonds.

The term sec(T-O-T) is the secant of the T-O-T bond angle; ⟨sec(T-O-T)⟩, the mean of four values over a tetrahedron.

$\langle T_j\text{-O}\rangle$ is the mean bond length of the second tetrahedron bonded to the oxygen atom; $\langle\langle T_j\text{-O}\rangle\rangle$, the mean over the four neighboring tetrahedra.

$|T|$ is the statistic for testing the null hypothesis that the corresponding coefficient is zero. It follows Student's t distribution.

2. The bonding of extraframework cations to the bridging oxygen tends to increase the T-O bond lengths. Brown et al. (1969) demonstrated that T-O bond lengths were correlated with the number of such cations bonded to the oxygen, and Fleet et al. (1966) demonstrated a dependence of T-O bond lengths upon M-O distances. These two terms are often combined in a sum to characterize the total bond-strength sum to the oxygen (e.g., Phillips et al., 1973; Wenk and Kroll, 1984; Geisinger et al., 1985).

3. An inverse correlation of T-O bond lengths with T-O-T angles has been demonstrated in framework silicates (e.g., Phillips et al., 1973; Wenk and Kroll, 1984; Geisinger et al., 1985), usually linearized by a function of the secant of the T-O-T angle.

4. Analyses of fully ordered framework structures have also suggested that a function of O-T-O angles is also correlated with T-O distances (Geisinger et al., 1985).

Wenk and Kroll (1984) improved the fit of calculated to observed T-O bond lengths by considering the deviation of individual distances from the mean values for each tetrahedron in four anorthites (An_{91}–An_{100}). This approach has the advantage of eliminating the effects of (Al, Si)-site occupancies from the analysis, whereas Phillips et al. (1973) had considered anorthite to be fully ordered. However, because they only considered anorthites with up to 9 mol% albite component, Wenk and Kroll (1984) were able to ignore the linkage factor (factor 1 in the previous section) in their analysis. Our more extensive database of $I\bar{1}$ structures, including both ordered and partially ordered anorthites with up to 32 mol% albite component, allows us to include this factor. Building on the previous work, we therefore chose the same dependent variable, (T-O)-⟨T-O⟩, as Wenk and Kroll (1984) in a series of regression analyses that were used to evaluate the significance of previously mentioned factors 1 through 4 in the refined $I\bar{1}$ structures.

Initial analyses of the T-O bond lengths from the $I\bar{1}$ refinements duplicated those of Wenk and Kroll (1984). When all 640 observations were treated as a single population, the estimated coefficients are within an esd of those found by Wenk and Kroll (1984). However, as the results reported in Table 7 demonstrate, the separate treatment of Al-rich and Si-rich tetrahedra (by the method of dummy variables) in this analysis results in a significant improvement in the fit of the regression. As previously demonstrated by Geisinger et al. (1985), we therefore conclude that these two populations of T-O bonds respond differently to both changes in the T-O-T angle and the bonding of other cations to the bridging oxygen, with the SiO_4 tetrahedra being the less responsive (i.e., stiffer). We then explored two further factors previously reported to be significant. The f_s (T) term of Geisinger et al. (1985) (equivalent to factor 4 previously mentioned) was found to be insignificant in the presence of the other terms, a result we attribute to the small range of O-T-O angles arising from averaging in the $I\bar{1}$ structures. The significance of the linkage factor was explored by the addition to the analysis of an independent variable of the form $\langle T_j\text{-O}\rangle - \langle\langle T_j\text{-O}\rangle\rangle$, where $\langle T_j\text{-O}\rangle$ is the mean bond length of the second tetrahedron to which the oxygen in question is bonded, and the second term is a mean taken over the four neighboring tetrahedra. It is interesting to note that this last is found to be statistically the same for both Al and Si tetrahedra, as was suggested by the results of MO calculations on $H_7T_2O_7$ clusters (Geisinger et al., 1985). The magnitude of the coefficient is equivalent to an individual T-O → Si bond being 0.30(1) Å longer than a T-O → Al bond in the $I\bar{1}$ structures. The net result of this analysis is that 84% of the deviations of individual T-O bond lengths from ⟨T-O⟩ values in $I\bar{1}$ anorthites can be accounted for by an equation whose coefficients are given in Table 7, with the residuals on the order of the esd's of the observed bond lengths.

The success of this regression equation in accounting for the factors that determine variations in T-O bond lengths can also be demonstrated by using the coefficients determined by regression analysis to remove the influence of the factors that affect individual T-O bond lengths. Observed T-O bond lengths were adjusted by subtracting the calculated effects of M-O bonding, T-O-T bond angle, and the occupancy of neighboring tetrahedra as measured by the $\langle T_j\text{-O}\rangle - \langle\langle T_j\text{-O}\rangle\rangle$ term already defined. The adjusted T-O bond lengths show greatly reduced variation within each tetrahedron compared to the variation in observed bond lengths. Root-mean-square deviations of bond lengths from ⟨T-O⟩ values, $\frac{1}{4}(\Sigma|(\text{T-O}) - \langle\text{T-O}\rangle|^2)^{1/2}$, are reduced from a range of 0.013–0.030 Å for observed bond lengths to a range of 0.002–0.013 Å (with the majority less than 0.006 Å) for the adjusted ones. Indeed, the differences between individual bond lengths within a tetrahedron are now comparable to the combined esd's associated with the experimental determination of a pair of individual bond lengths.

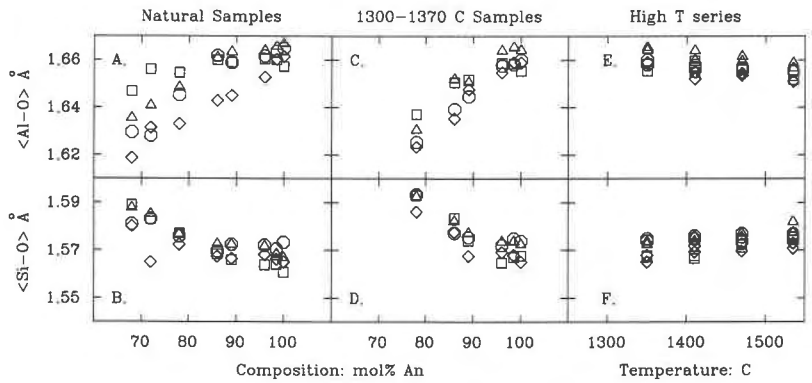

Fig. 5. The variation of adjusted mean tetrahedral bond distances, $\langle T\text{-}O\rangle_{adj}$, with composition and annealing temperature. (**A**, **B**) Natural samples. (**C**, **D**) Samples annealed at 1300–1370 °C. (**E**, **F**) Val Pasmeda and Monte Somma samples annealed at varying temperatures. Symbols as for Fig. 4.

The mean adjusted bond lengths of the tetrahedra, $\langle T\text{-}O\rangle_{adj}$, should reflect the effect of (Al, Si) site occupancy alone. It is therefore interesting to compare the trends in these corrected values with those already noted in the observed values. First, the grand structure means of the adjusted bond lengths, $\langle\langle T\text{-}O\rangle\rangle_{adj}$, are, like the observed values, invariant with the state of order and appear to vary linearly with bulk composition of the crystal. A linear regression yields the relationship

$$\langle\langle T\text{-}O\rangle\rangle_{adj} = 0.0212(12)n_{An} + 1.5935(11). \quad (3)$$

It should be noted that the slope of this line is only two thirds of the slope of the similar analysis of the uncorrected bond lengths (Eqs. 1 and 2). One third of the variation in observed grand mean bond lengths in $I\bar{1}$ feldspar structures is therefore attributable to factors other than variation in (Al,Si) content of the structure. Since the linkage factor is compensated internally within each tetrahedron, this difference must be due to effects related to (Ca,Na) substitution.

The variations of $\langle T\text{-}O\rangle_{adj}$ are presented as a function of composition in Figure 5. Comparison with the plot of uncorrected $\langle T\text{-}O\rangle$ values (Fig. 4) shows several significant differences. In the natural samples, only the T2oo site shows significant change in size from An_{100} to An_{86}; at more albite-rich compositions, all of the Si-rich sites show a small increase in size, whereas all of the Al-rich sites show varying degrees of contraction. These are different trends from those displayed by the uncorrected $\langle T\text{-}O\rangle$, and they would suggest an initial substitution of Si into the T2oo tetrahedron alone as the (Si:Al) ratio is increased from that in anorthite, followed by a general increase in (Al,Si) disorder beyond An_{86}. Preferential substitution of Si for Al on T2 sites has also been inferred from NMR measurements on these same samples (Kirkpatrick et al., 1987). The idea that increasing albite component is accommodated within $I\bar{1}$ structures by appropriate (Al,Si) exchange within the "An-like" portions of the plagioclase structure (e.g., Tagai et al., 1980; Wenk and Kroll, 1984) is therefore a simplification.

In the samples annealed at ~1300 °C, the difference between $\langle T1oz\text{-}O\rangle_{adj}$ and the remaining Al-rich tetrahedra (Fig. 5C) is much less pronounced than in the uncorrected $\langle T\text{-}O\rangle$ values, an effect also apparent in the high-temperature series of Val Pasmeda and Monte Somma samples (Fig. 5E). This may be attributed to the large effect, now corrected, that a change in the (Ca,Na) distribution has on the bonding environment of the Oa1z oxygen. From the samples annealed at different temperatures, it also appears that the T1oz and T2oo sites are slightly smaller, and hence less Al-rich, than T1mo and T2mz and that the T1mz and T2mo sites are enriched in Al relative to T1oo and T2oz.

States of order: Q_{OD}

The calibration of $\langle T\text{-}O\rangle_{adj}$ to give absolute (Al,Si)-site populations is beset by many of the same problems already noted by those attempting to derive (Al,Si) distributions from observed T-O bond lengths (e.g., Smith and Brown, 1988; Harlow and Brown, 1980; Kroll and Ribbe, 1983). Either the sizes of pure AlO_4 and pure SiO_4 tetrahedra must be known for the structure type under consideration, or some independent determination of (Al,Si) occupancies is needed. The only available neutron refinement of an $I\bar{1}$ feldspar that might give the required information about site occupancies is that of Tagai et al. (1980). Unfortunately, in this refinement, the (Al,Si) site occupancies were not constrained to correspond to the known composition; a cation-deficient microprobe analysis gave An_{66}, yet the refined site occupancies correspond to an overall composition of An_{78}.

By contrast, the evaluation of the state of order within these feldspars only requires an estimate of the *difference* in size between a pure Al site and a pure Si site. The linear dependence of $\langle\langle T\text{-}O\rangle\rangle_{adj}$ on composition implies that there is a linear relationship between mean T-O bond

Table 8. Order parameters for $I\bar{1}$ feldspars

Sample	⟨⟨Al-O⟩⟩ − ⟨⟨Si-O⟩⟩	Q_{OD}	Q_{OD}
Val Pasmeda	0.124	0.92	0.92
Val Pasmeda/3	0.118	0.87	0.87
Val Pasmeda/8	0.115	0.85	0.85
Val Pasmeda/7	0.111	0.82	0.82
Val Pasmeda/6	0.106	0.78	0.78
Monte Somma	0.123	0.91	0.92
Monte Somma/1	0.118	0.87	0.88
Monte Somma/8	0.112	0.83	0.84
Monte Somma/7	0.112	0.83	0.84
Monte Somma/6	0.108	0.80	0.81
115082a	0.119	0.88	0.90
115082a/1	0.117	0.87	0.89
87975a	0.115	0.85	0.90
87975a/1	0.103	0.76	0.81
21704a	0.115	0.85	0.92
21704a/1	0.092	0.68	0.73
101377a	0.097	0.72	0.81
101377a/1	0.065	0.48	0.55
Crystal Bay	0.087	0.65	0.75
Lake Co.	0.075	0.56	0.67

Note: The first value of Q_{OD} for each sample is with respect to $Q_{OD} = 1$ for fully ordered An_{100}. The second value is with resepct to $Q_{OD} = 1$ for the maximum possible order at each composition.

lengths adjusted for external influences and mean (Al,Si) occupancies. The compositional range from albite to anorthite corresponds to a change in mean occupancies from $Al_{0.25}Si_{0.75}$ to $Al_{0.50}Si_{0.50}$, so the difference between fully ordered Al and Si sites, ⟨Al-O⟩* − ⟨Si-O⟩*, is four times the slope of the regression line, or 0.0848(48) Å. The adjustments to T-O bond lengths calculated from the parameters derived in the regressions described above were found to be not applicable to $C\bar{1}$ structures, so the data for the regression of $\langle\langle T\text{-}O\rangle\rangle_{adj}$ versus composition only spans An_{68} to An_{100}. The precision in an estimate of ⟨Al-O⟩* − ⟨Si-O⟩* can be improved by using the observation that the trend in ⟨⟨T-O⟩⟩ is also linear with composition and spans the entire plagioclase solid solution. (Because both are linear with composition, the use of observed, rather than adjusted, bond lengths makes no difference to final estimates of Q_{OD}.) The estimate of ⟨Al-O⟩* − ⟨Si-O⟩* derived from the slope of Eq. 2 is thus 4 × 0.0338 = 0.135(2) Å.

A thermodynamic order parameter, Q_{OD}, for (Al, Si) ordering in pure anorthite (An_{100}) can be defined in terms of actual site occupancies in the usual way:

$$Q_{OD} = \langle Al\rangle_{Al} - \langle Al\rangle_{Si}, \quad (4)$$

where $\langle Al\rangle_{Al}$ is the average fractional occupancy by Al of the Al-rich sites and $\langle Al\rangle_{Si}$ is the average fractional occupancy by Al of the Si-rich sites (see Carpenter, 1988). If a linear relationship between ⟨T-O⟩ and site occupancies is assumed, Q_{OD} may be given directly in terms of the bond lengths:

$$Q_{OD} = K^{-1}(\langle\langle Al\text{-}O\rangle\rangle - \langle\langle Si\text{-}O\rangle\rangle), \quad (5)$$

where ⟨⟨Al-O⟩⟩ is the mean bond length of the four Al-rich sites in the $I\bar{1}$ structure, ⟨⟨Si-O⟩⟩ is the mean bond length of the four Si-rich sites, and $K = \langle Al\text{-}O\rangle^* - \langle Si\text{-}O\rangle^* = 0.135$ Å. Q_{OD} is thus normalized to vary between zero for a $C\bar{1}$ structure and unity for a fully ordered $I\bar{1}$ crystal.

The effect of composition can be incorporated into the definition of Q_{OD} in two alternative ways, depending on how the value for complete order is normalized. The same definition as used for pure anorthite, with $K = 0.135$ Å and observed ⟨T-O⟩ values, gives Q_{OD} with respect to complete order in An_{100} crystals. Crystals with intermediate compositions will have, as their maximum degree of order, all Si-rich sites fully occupied by Si and the remaining sites filled by Al + Si, giving $Q_{OD} < 1$. In the second description, these fully ordered states may be renormalized to $Q_{OD} = 1$ by making K dependent upon composition:

$$K = 0.0676(1 + n_{An}). \quad (6)$$

(The coefficient of 0.0676 is merely 2 × 0.0338, so as to still give $K = 0.135$ Å for An_{100}.) Values for Q_{OD} calculated in both ways for the full set of refined structures are given in Table 8. Contributions to the uncertainties in the estimates of Q_{OD} come from two sources. The esd of the constant K, derived from the esd of the slope of the regression line, amounts to about $0.04Q_{OD}$, or 0.02 to 0.035 for the values of Q_{OD} in these samples. The contribution from ⟨⟨Al-O⟩⟩ and ⟨⟨Si-O⟩⟩ is more difficult to assess, because it is not clear how the esd's of individual bond lengths should be propagated into mean values (see, for example, the discussion in Hazen and Finger, 1982). If we assign an esd typical of individual T-O bond lengths, 0.005 Å, to both ⟨⟨Al-O⟩⟩ and ⟨⟨Si-O⟩⟩ values, the net uncertainty in the order parameters is ~0.06 Q_{OD}. However, it is clear from examination of the values in Table 8 that the internal consistency in, for example, the two series of annealed samples, is of the order of 0.03 Q_{OD}.

Three qualitative conclusions may immediately be drawn from the observed ⟨⟨Al-O⟩⟩ − ⟨⟨Si-O⟩⟩ variations (Fig. 3) and the Q_{OD} values calculated from them (Table 8). First, the degree of order clearly diminishes systematically as albite is added in solid solution, both for the natural crystals and their heat-treated equivalents. The value of ⟨⟨Al-O⟩⟩ − ⟨⟨Si-O⟩⟩ extrapolates to zero, i.e., to $Q_{OD} = 0$, in Figure 3 at compositions that are consistent with the position of the $C\bar{1}$–$I\bar{1}$ transition line determined experimentally by Carpenter and McConnell (1984). Second, Val Pasmeda anorthite, with $Q_{OD} = 0.92$, has some (Al,Si) disorder between tetrahedral sites and is not fully ordered as is commonly assumed (e.g., Phillips et al., 1973). Finally, heat treatments at 1300 °C and above induce significant disorder, consistent with previous crystallographic studies of annealed crystals (Bruno et al., 1976; Facchinelli et al., 1979; Chiari et al., 1984).

Carpenter (1988) has outlined a preliminary thermodynamic description of the $C\bar{1}$–$I\bar{1}$ transition. A more rigorous analysis, based upon the new data set, will be presented elsewhere. For present purposes, it may be of interest to compare the estimates of Q_{OD} from previously

published refinements (Table 1 of Carpenter, 1988) with the values given here (Table 8). The definition of Q_{OD} used by Carpenter (1988) corresponds to the second definition above, namely $Q_{OD} = 1$ for maximum order at each composition. The values are broadly similar but show numerical discrepancies.

A limitation of the use of a fixed value for ⟨Al-O⟩* − ⟨Si-O⟩* in describing Q_{OD} is illustrated by estimating the degree of order in albite with our value. Following Carpenter (1988), Q_{OD} for ordering under $C\bar{1}$ symmetry in albite may be expressed as

$$Q_{OD} = K^{-1}(\langle T1o\text{-}O\rangle - \langle T1m - O\rangle). \quad (7)$$

With $K = 0.135$ Å, Equation 7 gives Q_{OD} from 0.97 to 1.01 for the four low albite structures tabulated by Kroll and Ribbe (1983). An independent value for Amelia albite has been obtained from neutron-diffraction data and is 0.92 ± 0.04 (Harlow and Brown, 1980; and see Carpenter, 1988). At the same time, Q_{OD} is 0.05 and 0.07 for two end-member high albite structures listed by Kroll and Ribbe (1983), whereas both should probably display $Q_{OD} = 0$. At high temperature, Q_{OD} defined in the same way can appear to vary even though kinetic considerations suggest that there was insufficient time during experiments for reordering to occur (see high-temperature data of Prewitt et al., 1976, on a high albite). It is clear again, therefore, that while grand-mean values of the bond lengths may vary systematically, the mean values for individual tetrahedra are modified significantly by effects other than (Al,Si) content. In this case, distortions associated with the $C2/m$–$C\bar{1}$ displacive transition may be a contributing factor.

Conclusions

By collecting data from a suite of well-characterized anorthite-rich plagioclase feldspars we have been able to demonstrate several important trends and reach conclusions about the $I\bar{1}$ feldspar structures previously obscured by problems associated with interlaboratory comparisons:

1. Careful study of the relationship between various structure-refinement models for $I\bar{1}$ feldspars demonstrates that the results obtained for bond lengths and angles are model dependent. Comparisons cannot confidently be made between structural parameters obtained from different models. In particular, previously reported discontinuities in grand-mean tetrahedral bond lengths, ⟨⟨T-O⟩⟩, with composition have been shown to arise from just such a comparison.

2. The large-cation sites occupied by Na and Ca show a split character apparently identical to that observed in average structure determinations of $P\bar{1}$ structures, even at compositions for which the *c* and *d* reflections characteristic of $P\bar{1}$ symmetry are either very diffuse or absent.

3. The orientation of many of the "thermal ellipsoids" of the framework atoms in $I\bar{1}$ average structures of anorthite-rich crystals reflects the orientation of the split vector of the corresponding atom pairs in the true $P\bar{1}$ structures. These ellipsoids retain the same orientation across the entire composition range that we have studied. Whether this implies that all $I\bar{1}$ structures have local $P\bar{1}$ symmetry and one observes a space average by X-ray diffraction, or whether the more albite-rich crystals are displaying large-amplitude vibrational modes that parallel the displacements associated with a $I\bar{1}$–$P\bar{1}$ transition (a time average), cannot be determined by X-ray diffraction experiments.

4. The observed mean tetrahedral bond lengths, ⟨T-O⟩, do not reflect (Al,Si) occupancies alone, but are perturbed by M-O bonding, T-O-T bond angles, and a linkage factor dependent upon neighboring tetrahedral sites. When corrected for these external factors, the sizes of the tetrahedra show significantly different trends from those associated with uncorrected raw ⟨T-O⟩ bond lengths. The previously proposed model of the substitution of Si into, and redistribution of Al within "anorthite-like" portions of the $I\bar{1}$ structure is thus seen to be a simplification arising from the interpretation of ⟨T-O⟩ data perturbed by factors other than (Al,Si) occupancies.

5. The state of order within the $I\bar{1}$ phase, measured by Q_{OD}, may be obtained from the difference between the mean bond lengths of all of the Al-rich and all of the Si-rich tetrahedra. The results indicate that the best-ordered anorthite still contains some 8% (Al, Si) disorder.

Acknowledgments

X-ray diffraction experiments were supported by NSF grants EAR86-18649 to C. T. Prewitt and L.W.F., by EAR86-18602 to C. T. Prewitt, and by EAR84-19982 to L.W.F. and R. M. Hazen. R.J.A. gratefully acknowledges the receipt of Research Fellowships from the Carnegie Institution of Washington and the Royal Society, and M.A.C. the receipt of a Research Fellowship from the Nuffield Foundation, and financial support from the Natural Environment Research Council of Great Britain (grant no. GR3/5547). We would like to thank Nancy Ross for her assistance in all phases of this study, and J. V. Smith and C. W. Burnham for reviews of the manuscript.

References cited

Becker, P.J., and Coppens, P. (1974) Extinction within the limit of validity of the Darwin transfer equations. I. General formalisms for primary and secondary extinction and their application to spherical crystals. Acta Crystallographica, A30, 129–147.

Berking, B. (1976) Die Verfeinerung der Kristallstruktur eines lunaren Plagioklases An_{90}. Zeitschrift für Kristallographie, 144, 189–197.

Brown, G.E., Gibbs, G.V., and Ribbe, P.H. (1969) The nature and variation in length of the Si-O and Al-O bonds in framework silicates. American Mineralogist, 54, 1044–1061.

Bruno, E., Chiari, G., and Facchinelli, A. (1976) Anorthite quenched from 1530°C. I. Structure refinement. Acta Crystallographica, B32, 3270–3280.

Burnham, C.W. (1966) Computation of absorption corrections, and the significance of end effects. American Mineralogist, 51 159–167.

Carpenter, M.A. (1988) Thermochemistry of aluminium/silicon ordering in feldspar minerals. In E. Salje, Ed., Physical properties and thermodynamic behaviour of minerals. NATO ASI series C, 225, 265–323. Reidel, Dordrecht, Netherlands.

Carpenter, M.A., and McConnell, J.D.C. (1984) Experimental delineation of the $C\bar{1}$–$I\bar{1}$ transformation in intermediate plagioclase feldspars. American Mineralogist, 69, 112–121.

Carpenter, M.A., McConnell, J.D.C., and Navrotsky, A. (1985) Enthalpies of ordering in the plagioclase feldspar solid solution. Geochimica et Cosmochimica Acta, 49, 947–966.

Chiari, G., Benna, P., and Bruno, E. (1984) The structure of bytownite (An_{85}). A new refinement. Zeitschrift für Kristallographie, 169, 35–49.

Czank, M. (1973) Struckturuntersuchungen von Anorthit im Temperaturbereich von 20°C bis 1430°C. Dissertation, ETH, Zürich.

Facchinelli, A., Bruno, E., and Chiari, G. (1979) The structure of bytownite quenched from 1723K. Acta Crystallographica, B35, 34–42.

Finger, L.W., and Prince, E. (1975) A system of Fortran IV computer programs for crystal structure computations. NBS Technical Note 854.

Fleet, S.G., Chandrasekhar, S., and Megaw, H.D. (1966) The structure of bytownite ("body-centred anorthite"). Acta Crystallographica, 21, 782–801.

Geisinger, K.L., Gibbs, G.V., and Navrotsky, A. (1985) A molecular orbital study of bond length and angle variations in framework silicates. Physics and Chemistry of Minerals, 11, 266–283.

Harlow, G.E., and Brown, G.E. (1980) Low albite: An X-ray and neutron diffraction study. American Mineralogist, 65, 986–995.

Hazen, R.M., and Finger, L.W. (1982) Comparative crystal chemistry. Wiley, New York.

International tables for X-ray crystallography. (1974) Kynoch Press, Birmingham.

Kalus, C. (1978) Neue Struckturbestimmung des Anorthits unter Berücksichtigung möglicher Alternativen. Dissertation. Universität München.

Kempster, C.J.E., Megaw, H.D., and Radoslovich, E.W. (1962) The structure of anorthite, $CaAl_2Si_2O_8$. I. Structure analysis. Acta Crystallographica, 15, 1005–1017.

King, H., and Finger, L.W. (1979) Diffracted beam crystal centring and its application to high-pressure crystallography. Journal of Applied Crystallography, 12, 374–378.

Kirkpatrick, R.J., Carpenter, M.A., Yang, W.H., and Montez, B. (1987) ^{29}Si magic-angle NMR spectroscopy of low-temperature ordered plagioclase feldspars. Nature, 325, 236–237.

Kroll, H. (1983) Lattice parameters and determinative methods for plagioclase and ternary feldspars. In Mineralogical Society of America Reviews in Mineralogy, 2, 101–119.

Kroll, H., and Ribbe, P.H. (1983) Lattice parameters, composition, and Al/Si order in alkali feldspars. In Mineralogical Society of America Reviews in Mineralogy, 2, 57–99.

Megaw, H.D. (1956) Notation for feldspar structures. Acta Crystallographica, 9, 56–60.

Megaw, H.D., Kempster, C.J.E., and Radoslovich, E.W. (1962) The structure of anorthite, $CaAl_2Si_2O_8$. II. Description and discussion. Acta Crystallographica, 15, 1017–1035.

Phillips, M.W., and Ribbe, P.H. (1973) The variation of tetrahedral bond lengths in sodic plagioclase feldspars. Contributions to Mineralogy and Petrology, 39, 327–339.

Phillips, M.W., Ribbe, P.H., and Gibbs, G.V. (1973) Tetrahedral bond length variations in anorthite. American Mineralogist, 58, 495–499.

Prewitt, C.T., Sueno, S., and Papike, J.J. (1976) The crystal structures of high albite and monalbite at high temperatures. American Mineralogist, 61, 1213–1225.

Redfern, S.A.T., and Salje, E. (1987) Thermodynamics of plagioclase II: Temperature evolution of the spontaneous strain at the $I\bar{1}$–$P\bar{1}$ phase transition in anorthite. Physics and Chemistry of Minerals, 14, 184–195.

Redfern, S.A.T., Graeme-Barber, A., and Salje, E. (1988) Thermodynamics of plagioclase III: Spontaneous strain at the $I\bar{1}$–$P\bar{1}$ phase transition in Ca-rich plagioclase. Physics and Chemistry of Minerals, 16, 157–163.

Ribbe, P.H. (1983) Chemistry, structure, and nomenclature of feldspars. In Mineralogical Society of America Reviews in Mineralogy, 2, 1–20.

Salje, E. (1985) Thermodynamics of sodium feldspar I: Order parameter treatment and strain induced coupling effects. Physics and Chemistry of Minerals, 12, 93–98.

——— (1987) Thermodynamics of plagioclase I: Theory of the $I\bar{1}$–$P\bar{1}$ phase transition in anorthite and calcium-rich plagioclases. Physics and Chemistry of Minerals, 14, 181–188.

Salje, E., and Wruck, B. (1988) Kinetic rate laws derived from order parameter theory II: Interpretation of experimental data by Laplace-transformation, the relaxation spectrum, and kinetic gradient coupling between two order parameters. Physics and Chemistry of Minerals, 16, 140–147.

Salje, E., Kuscholke, B., Wruck, B., and Kroll, H. (1985) Thermodynamics of sodium feldspar II: Experimental results and numerical calculations. Physics and Chemistry of Minerals, 12, 99–107.

Smith, J.V. (1954) A review of the Al-O and Si-O distances. Acta Crystallographica, 7, 479–483.

Smith, J.V., and Bailey, S.W. (1963) Second review of Al-O and Si-O tetrahedral distances. Acta Crystallographica, 16, 801–811.

Smith, J.V., and Brown, W.L. (1988) Feldspar minerals, vol. 1. Crystal structures, physical, chemical, and microstructural properties. Springer-Verlag, New York.

Smyth, J.R. (1986) Crystal structure refinement of a lunar anorthite, An_{94}. Journal of Geophysical Research, 91, E91–E97.

Tagai, T., Joswig, W., Korekawa, M., and Wenk, H.R. (1980) Die bestimmung der Al/Si-verteilung mittels Neutronenbeugung in einem Plagioklas An_{68}. Zeitschrift für Kristallographie, 151, 77–89.

Wainwright, J.E., and Starkey, J. (1971) A refinement of the structure of anorthite. Zeitschrift für Kristallographie, 133, 75–84.

Wenk, H.R., and Kroll, H. (1984) Analysis of $P\bar{1}$, $I\bar{1}$ and $C\bar{1}$ plagioclase structures. Bulletin de Minéralogie, 107, 467–487.

Manuscript received June 12, 1989
Manuscript accepted September 7, 1989